Journal of Computational Physics 426 (2021) 109947

Contents lists available at ScienceDirect

Journal of Computational Physics

www.elsevier.com/locate/jcp

Entropy stable boundary conditions for the Euler equations

Magnus Svärd

Department of Mathematics, University of Bergen, Postbox 7800, 5020 Bergen, Norway

ARTICLE INFO

Article history:
Received 12 June 2020
Received in revised form 18 September 2020
Accepted 22 October 2020
Available online 4 November 2020

Keywords:
Entropy stability
Boundary conditions
Euler equations
Navier-Stokes equations

ABSTRACT

We consider the initial-boundary value Euler equations with the aim to derive boundary conditions that yield an entropy bound for the physical (Navier-Stokes) entropy. We begin by reviewing the entropy bound obtained for standard no-penetration wall boundary conditions and propose a numerical implementation. The main results are the derivation of full-state boundary conditions (far-field, inlet, outlet) and the accompanying entropy stable implementations. We also show that boundary conditions obtained from linear theory are unable to bound the entropy and that non-linear bounds require additional boundary conditions. We corroborate our theoretical findings with numerical experiments.

1. Introduction

In aerodynamic simulations with the Euler and Navier-Stokes equations, the boundary conditions play an important role for a number of interconnected reasons. i) Mathematically, boundary conditions have to be well-posed, i.e., lead to a bounded and unique solution. This pertains to both the structure and the number of necessary and sufficient conditions. (See [7].) ii) Their numerical approximations have to be stable in conjunction with the interior scheme. iii) They should be an accurate model of the physics at the boundary. All three conditions are required for a successful simulation.

For exterior flow problems, the two most common boundary conditions are wall and far-field boundaries. At a wall, a viscous fluid clings to the wall such that the velocity on the wall is zero (no-slip). That is, the physical model is given and, with the use of no-slip and a (Dirichlet or Neumann) condition on temperature, it turns out that linear well-posedness as well as linear numerical stability of the Navier-Stokes equations follow. (See e.g. [18].) Furthermore, no-slip and a Neumann condition on temperature also lead to non-linear estimates. (See [5].)

Although, the no-slip boundary condition is (to a good approximation) observable in nature, it turns out that only the wall normal component of the velocity is zero for inviscid fluids (the Euler equations) or else too many boundary conditions are given.

At far-field boundaries, the idea is that sufficiently far away from any object that perturbs the freestream, the solution should approach the constant freestream. Linearly well-posed and linearly stable far-field conditions have been proposed in e.g., [10,12,11,8,15,13] for the Navier-Stokes equations. These are Navier-Stokes modifications of the characteristic boundary conditions commonly used for the Euler equations.

Successful as the linear theory has been, it does not provide a complete mathematical description. Linearly stable boundary conditions are obtained by linearising around a smooth solution which determines the characteristic directions at the boundary. When applying the linear theory to the non-linear problem there is an obvious problem: The solution state at the boundary, i.e., the trace, and the freestream state that provides data to the boundary conditions are generally differ-

E-mail address: Magnus.Svard@math.uib.no.

https://doi.org/10.1016/j.jcp.2020.109947

ent. Hence, the speed and directions of the waves at the boundaries are not uniquely defined. (A practical solution of this problem is to e.g. use the Roe average between the two competing boundary states to define the wave speeds, [15].) Nevertheless, boundary conditions derived from linear theory often work well.

For interior flows, such as flows in ducts, there are typically inlets, outlets and wall boundary conditions. One way to model inlets and outlets, is to use characteristic boundary conditions, which is mathematically equivalent to the far-field treatment, since only the boundary data differ. (Instead of constant freestream values one may want to provide varying profiles for the variables.) This procedure is linearly well-posed as long as the inlet or outlet velocities are locally parallel to the adjacent walls. (For inviscid flows.) This condition is termed *compatibility of boundary conditions* and is necessary to maintain continuity of the solution. (See [6].)

The defining feature of characteristic boundary conditions, whether used at far-field, inlet or outlet, is that they draw information from a completely defined boundary-data vector of which only a subspace is enforced. (Unless all characteristics are pointing into the domain (supersonic inflow), then the full state is enforced.) Herein, we will use the collective term *full-state boundary condition* for any boundary condition that draws information from a completely defined reference state.

Remark. We acknowledge that it may in practice be difficult to obtain data for all variables but that is nevertheless needed for well-posedness of characteristic-type conditions. To alleviate this requirement, a pressure boundary condition is sometimes used at outlets, which can be shown to be marginally linearly well-posed ([15]), but its non-linear stability is unknown and we have chosen not to consider it here.

Lately, there has been an increasing interest to extend the stability theory of numerical schemes to allow non-linear estimates of the solutions. One such choice, is entropy stability, where the numerical schemes are designed to bound one or more entropies. (See the review paper [21] for initial-value conservation laws.)

The closure of entropy stable schemes at the boundaries has been addressed to much lesser extent. For viscous and inviscid walls, one can consult e.g. [20,14,16]. For far-field boundaries, few attempts have been made. In [17] entropy stable characteristic-type boundary conditions for the Euler equations are proposed. However, the entropy stability in [17] refers to a generalised entropy that is not available for the Navier-Stokes equations. In [20] the Navier-Stokes entropy was considered, but assumptions on the structure of the Jacobian eigensystem were made and in [4] a priori known L^∞-bounds on temperature and the inverse of density were needed.

In this paper, we consider the Euler equations and the Navier-Stokes entropy. At first in one space dimension and we review the entropy stability of no-penetration wall boundary conditions. Furthermore, we propose full-state boundary conditions that are entropy stable with respect to an affine rescaling of the Navier-Stokes entropy. (Hence, a generalisation to the Navier-Stokes system is possible.) We unify the entropies used for wall and full-state boundary such that both types of boundaries can appear in the same problem. Next, we propose entropy stable numerical implementations of walls and full-state boundary conditions in one space dimension. Then we turn to the two-dimensional case to demonstrate how to generalise the theory. To this end, we use a two-dimensional finite-volume scheme and prove entropy stability for the initial-boundary value Euler equations. (The procedure is applicable to schemes other than finite volume.) Furthermore, we discuss how to handle general full-state boundary conditions including inlets and outlets. Finally, we demonstrate the robustness of the proposed conditions in a few numerical simulations. The extension to Navier-Stokes systems is postponed to a future article as it requires considerable attention to the interior discretisation of the viscous terms.

2. Entropy

We consider the Euler equations of gas dynamics, which is an example of a conservation law,

$$u_t + f(u)_x = 0, \tag{1}$$

where u are the conservative variables and f is the flux function. In the specific case of gas dynamics, we have,

$$u = (\rho, \rho v, E)^T,$$
$$f(u) = (\rho v, \rho v^2 + p, v(E+p))^T$$

where $E = \frac{p}{\gamma - 1} + \frac{\rho v^2}{2}$ is the total energy and γ is the adiabatic constant. Furthermore, ρ, v, p is the density, velocity and pressure and we assume the ideal gas law, $p = \rho R T$.

An entropy function is a convex function, $U(u)$, that has an associated entropy flux $F(u)$ that satisfies $F_u = U_u f_u$. The entropy variables are $w^T = U_u$ and $\Psi(w) = < w, f(w) > - F(w)$ is the entropy potential. Furthermore, $f(w) = \Psi_w$.

Remark. To reduce the number of symbols, we abuse notation by writing e.g., $f(w) = f(u(w))$.

Admissible, possibly non-smooth, but (sufficiently) bounded, solutions, must satisfy the entropy inequality,

$$U(u)_t + F(u)_x \leq 0, \tag{2}$$

in a distributional sense. Since we aim to extend the theory to the Navier-Stokes equations, we are forced to consider the entropy $U(u) = -\rho S$, where $S = \log(p/\rho^\gamma)$ is the specific entropy and the associated entropy function $F = vU = -\rho v S = -mS$ (where $m = \rho v$ is the momentum). For this entropy, the entropy potential is $\Psi = (\gamma - 1)m$ and the entropy variables are,

$$w^T = \frac{1}{c_v}\left(-(S-\gamma) - \frac{v^2}{2T},\ \frac{v}{T},\ \frac{-1}{T}\right),$$

where c_v is the specific heat at constant volume. However, any affine transformation of the entropy is still an entropy of the Navier-Stokes system. Hence, we introduce

$$\tilde{U}(u) = U(u) - U(u_r) - U_u(u_r)(u - u_r), \tag{3}$$

where u_r is an a priori defined reference function. The new entropy variables are,

$$\tilde{w}^T = \tilde{U}_u = U_u(u) - U_u(u_r) = w^T(u) - w^T(u_r). \tag{4}$$

Furthermore, it is easy to verify that convexity of $\tilde{U}$ follows from convexity of U_{uu}: $\tilde{U}_{uu} = (U_u(u) - U_u(u_r))_u = U(u)_{uu}$. The corresponding entropy function and entropy potential are determined as follows:

$$\tilde{F}_u = \tilde{U}_u f_u = U_u f_u - U_u(u_r) f_u = F_u - U_u(u_r) f_u \tag{5}$$

such that,

$$\tilde{F} = F - U_u(u_r) f = F(u) - w(u_r)^T f(u) \tag{6}$$

and

$$\tilde{\Psi} = < \tilde{w}, f(w) > - \tilde{F} = < w - w(u_r), f(w) > - (F(u) - w(u_r)^T f(u)) = \Psi. \tag{7}$$

Finally, none of the above derivations concern variation in the (x, t)-space and we conclude that the reference function can be $u_r = u_r(x, t)$.

2.1. Wall

At a wall, the physically relevant boundary condition for the Euler equations is the so-called no-penetration boundary condition. That is, the normal component of the velocity is zero such that there is no convection through the wall. Here, we initially consider the domain $[0, 1]$ with wall at both ends, implying that $v(\{0, 1\}, t) = 0$. Upon integration of (2), we obtain,

$$\int_0^1 U_t\, dx + F(u(1,t)) - F(u(0,t)) \leq 0. \tag{8}$$

Seeing that $F = -mS$, both boundary terms vanish due to the boundary conditions and we obtain,

$$\int_0^1 U_t\, dx \leq 0.$$

Remark. We will consider multiple space dimensions below, but make the following preemptive remark: In multiple dimensions, there are multiple entropy fluxes, $F_i = \rho v_i S$, where v_i is a Cartesian velocity component. After integration in space, boundary terms of the form, $(n_1, n_2, n_3) \cdot (F_1, F_2, F_3)$ (where n_i are the components of wall normal) are obtained in the expression corresponding to (8). These vanish if the normal velocity is zero. (We reiterate, that it is well-known that the no-penetration condition bounds this entropy.)

Next, we consider the effect of the affine modification of the entropy given in (3). In analogy with (8), we obtain, $\int_0^1 \tilde{U}_t\, dx + \tilde{F}(u(1,t)) - \tilde{F}(u(0,t)) \leq 0$, where $\tilde{F} = F(u) - w(u_r)^T f(u)$. Inserting the boundary condition $v = 0$, yields, $\tilde{F} = -\frac{v_r}{c_v T_r} p$, where the subscript r denotes the value of the reference function. T_r and p are positive for admissible solutions, and the sign of the boundary terms depends both on the sign of v_r and the normal. We conclude that only reference functions with $v_r = 0$ at a wall, bound the entropy independently of the wall normal direction.

2.2. Full-state boundary condition

In 1-D there is no principle difference between a far-field, inlet or outlet when the full reference state is given. Hence, the discussion in this section applies generally to any full-state boundary conditions.

We begin by summarising the linearly well-posed characteristic boundary conditions that are commonly used at far-fields. That is, only the in-going characteristic waves are specified using the complete freestream state u_∞ given by ρ_∞, p_∞ and v_∞. The Euler equations (1) are linearised and symmetrised (see [1]) and a system of the form,

$$q_t + \mathcal{A} q_x = 0, \quad 0 < x < 1 \tag{9}$$

is obtained. q is the vector of symmetrised variables representing a perturbation around a (constant) freestream and $\mathcal{A} = \mathcal{A}_\infty$ is given by the freestream values. The energy rate is given by

$$\|q\|_t^2 + q^T \mathcal{A}_\infty q|_0^1 = 0$$

where $\|q\|^2 = \int_0^1 q^T q \, dx$. The following boundary conditions lead to an energy bound for the linearised equation (9),

$$\begin{aligned} &\mathcal{A}_\infty^+ q(0,t) = 0, \\ &\mathcal{A}_\infty^- q(1,t) = 0. \end{aligned} \tag{10}$$

That is the in-going characteristics are set to zero. $\mathcal{A}_\infty^{+/-}$ are the matrices obtained by splitting $\mathcal{A}_\infty$ according to the sign of the eigenvalues and $\mathcal{A}_\infty = \mathcal{A}_\infty^+ + \mathcal{A}_\infty^-$. The eigenvalues appearing in $\mathcal{A}_\infty$ are the well-known $v_\infty + c_\infty$, v_∞, $v_\infty - c_\infty$, where c_∞ is the freestream sound speed. Hence, the linear theory dictates that the following number of boundary conditions are provided:

- 3 at supersonic inflows (5 in 3D),
- 2 at subsonic inflows (4 in 3D),
- 1 at subsonic outflows (1 in 3D),
- 0 at supersonic outflows (0 in 3D).

Since the characteristics correspond to modes of the solution (of the linearised problem), it follows that these are the least number of boundary conditions necessary for an energy estimate and linear well-posedness. (See [6] for general linear well-posedness theory of initial-boundary value problems and [15] for more details on the above procedure for the Euler equations.)

The data in (10) are zero since the perturbations are (ideally) zero at the freestream. A non-linear rendering of these boundary conditions (used in practice) is to, e.g., compute the Roe-averaged flux Jacobian, $A(u(\{0,1\},t), u_\infty)$, and use the boundary conditions $A^{+/-} u(\{0,1\},t) = A^{+/-} u_\infty$. This procedure linearises to (10) (but so do other choices). (For more details on this procedure, consult e.g. [15].)

Turning to the entropy, we have as before,

$$\int_0^1 U_t \, dx + F(u(1,t)) - F(u(0,t)) \leq 0.$$

Suppose that we provide boundary conditions according to linear theory. Then, at supersonic inflows, F is completely determined by the freestream state and results in a bound on U. However, at a supersonic outflow, no boundary condition should be given and we do not obtain an entropy bound since $F = -\rho v S$ is indefinite. We conclude that the linear theory does not lead to a bound on the entropy.

Before we address entropy stability of full-state boundaries, we state some general relations that are valid for any entropy-pair. (These can be found in e.g. [21].) We denote flux Jacobian $f_u = A$, and the Roe-averaged Jacobian as A_{21}, such that

$$A_{21} \Delta u_{21} = f(u_2) - f(u_1) \tag{11}$$

where $u_{1,2}$ are two states and $\Delta u_{21} = u_2 - u_1$.

Next, we denote the solution state at $x = 0$ with a subscript 0 and the boundary data as u_g. That is, $w(u(0,t)) = w_0$ and $w(u_g(0,t)) = w_g$ and consider a straight line through phase space between w_g and w_0, i.e., $w(\xi) = \bar{w} + \xi \Delta w_{0g}$, where $\Delta w_{0g} = (w_0 - w_g)$, $\bar{w} = (w_0 + w_g)/2$, and $\xi \in [-1/2, 1/2]$. Then we define

$$H_{0g} = \int_{-1/2}^{1/2} u_w(w(\xi)) \, d\xi$$

such that

$$\Delta u_{0g} = H_{0g} \Delta w_{0g} \tag{12}$$

holds for our particular path through phase space. Consequently,

$$B_{0g} \Delta w_{0g} = f(u_0) - f(u_g)$$

where

$$A_{0g} = B_{0g} H_{0g}^{-1} \quad \text{(the Roe-average)} \tag{13}$$

and therefore,

$$B_{0g} = \int_{-1/2}^{1/2} f_w(w(\xi))\, d\xi. \tag{14}$$

Proposition 2.1. *Consider the Euler equations (1) on the domain* $[0, 1]$. *Let* u_g *be the data vector in the conservative variables. Define the matrix,*

$$R_{0g} = \int_{-1/2}^{1/2} \xi\, f_{\tilde{w}}\, d\xi, \tag{15}$$

where the path is the straight line between $\tilde{w}_g$ *and* $\tilde{w}_0$, *and* $\tilde{w}$ *are the entropy variables of the entropy (3) with* $u_r = u_g$ *(extended to* $[0, 1]$*). Then the full-state boundary condition,*

$$A_{0g}^{+}(u_0 - u_g) + R_{0g}^{+} H_{0g}^{-1}(u_0 - u_g) = 0 \tag{16}$$

(and analogously for $x = 1$*) leads to a bounded entropy.*

Proof. The proof is constructive and demonstrates how to deduce the boundary conditions (16). Hence, we begin by integrating the standard entropy inequality in space to arrive at (8). (To reduce notation, we only consider the boundary $x = 0$.) In order to bound the right-hand side of (8), we add and subtract F_g and then proceed to find conditions that bound $F_0 - F_g$. (The remaining F_g is bounded and will only contribute with a limited growth of $\tilde{U}$.)

Recall that $F(w) =< w, f(w) > -\Psi$ and $\Psi_w = f(w)$, and consider,

$$F(u_0) - F(u_g) = F(w_0) - F(w(u_g)) = \int_g^0 F_w\, dw = \int_g^0 < w, f(w) >_w - \Psi_w\, dw =$$

$$\int_g^0 f(w) + < w, f_w > - f(w)\, dw = \int_g^0 < w, f_w > dw$$

Using the specific linear path, we obtain

$$\int_g^0 < w, f_w > dw = \int_{-1/2}^{1/2} < w, f_w > \frac{dw}{d\xi} d\xi = \int_{-1/2}^{1/2} < w, f_w > \Delta w_{0g} d\xi \tag{17}$$

Next, we insert $w(\xi)$ into the last expression

$$\int_{-1/2}^{1/2} < \bar{w} + \xi \Delta w_{0g}, f_w > \Delta w_{0g} d\xi =$$

$$\frac{w_0}{2} \int_{-1/2}^{1/2} f_w\, d\xi \Delta w_{0g} + \frac{w_g}{2} \int_{-1/2}^{1/2} f_w\, d\xi \Delta w_{0g} + \Delta w \int_{-1/2}^{1/2} \xi\, f_w\, d\xi \Delta w_{0g} \tag{18}$$

Using (14), we identify the first term of (18) as

$$\frac{w_0}{2}\int_{-1/2}^{1/2} f_w\, d\xi\, \Delta w_{0g} = \frac{w_0}{2}(f(u_0) - f(u_g)). \tag{19}$$

At this point, we note that it is difficult to form quadratic terms that can be used to deduce stable boundary conditions. The way forward is to choose and affine entropy (3) rescaled with the boundary data, $u_r = u_g$. That is,

$$\tilde{U} = U(u) - U(u_g) - U'(u_g)(u - u_g) \tag{20}$$

and use the relations (4), (5), (6) and (7) to obtain the following identities,

$$\begin{aligned} \tilde{w}_0 &= w(u_0) - w(u_g) = \Delta w_{0g}, \\ \tilde{w}_g &= w(u_g) - w(u_g) = 0, \\ \Delta\tilde{w}_{0g} &= (\tilde{w}_0 - \tilde{w}_g) = \Delta w_{0g}. \end{aligned} \tag{21}$$

Returning to the derivation above, it is valid for the new entropy as well. That is, (19) turns into,

$$\frac{\tilde{w}_0}{2}\int_{-1/2}^{1/2} f_{\tilde{w}}\, d\xi\, \Delta\tilde{w} = \frac{\tilde{w}_0}{2}(f(u_0) - f(u_g)).$$

Using (21) and the Roe average (11) between the states u_0 and u_g, we obtain

$$\frac{\tilde{w}_0}{2}(f(u_0) - f(u_g)) = \frac{\Delta w_{0g}}{2}(f(u_0) - f(u_g)) = \frac{\Delta w_{0g}}{2}A_{0g}(u_0 - u_g). \tag{22}$$

Inserting the boundary condition (16), and using the relations (13) and (12), lead to

$$\begin{aligned} \frac{\Delta w_{0g}}{2}A_{0g}(u_0 - u_g) = \frac{\Delta w_{0g}}{2}(-R^+_{0g}H^{-1}_{0g} + A^-_{0g})(u_0 - u_g) = \\ \frac{1}{2}\Delta w_{0g}(-R^+_{0g} + B^-_{0g})\Delta w_{0g} \le 0 \end{aligned} \tag{23}$$

Next, we note that $\tilde{w}_g = 0$ in (18) thanks to (21), and we are left with

$$\Delta\tilde{w}_{0g}\int_{-1/2}^{1/2} \xi\, f_{\tilde{w}}\, d\xi\, \Delta\tilde{w}_{0g} = \Delta w_{0g}\int_{-1/2}^{1/2} \xi\, f_{\tilde{w}}\, d\xi\, \Delta w_{0g} = \Delta w_{0g} R \Delta w_{0g}. \tag{24}$$

In the same spirit as in (23), we split $R = R^+ + R^-$ and use the boundary condition (16) to obtain non-positive terms. □

The boundary condition (16), need not be the least intrusive since we do not know that it is the least number of boundary conditions. However, it is debatable if the principle of "least number of boundary conditions" has any meaning in the non-linear case. In the linear case, the wave speeds are a priori given and are neither affected by the boundary data nor the solution. Then it is clear that uniqueness is violated (at the boundary) if too many boundary conditions are specified since the trace will in general not match the boundary data.

In the non-linear case it looks like (16) is similar to the linear characteristic boundary conditions since A^+ and R^+ seem to extract a subset of the boundary data and not indiscriminately enforce the full state. However, the structure of A^+ and R^+, including how many waves to supply boundary conditions to, depend on both the trace of the solution and the boundary data in a non-linear feedback loop. In fact, *the A^+ and R^+ can not be computed without knowledge of the full-state boundary data.* Hence, neither (16) nor the non-linear renderings of (10) enforce the number of boundary conditions suggested by linear theory (listed above). *They both use 3 conditions (5 in 3D).* However, (16) is not a standard Dirichlet condition, but it rather enforces different subspaces of u_g with different weights.

2.3. Compatibility of walls and full-state boundaries

The wall boundary treatment discussed in Section 2.1, bounds the standard entropy, $U = -\rho S$ and the rescaled entropy (3) as long as the reference velocity is zero at the wall boundary. On the other hand, the full-state boundary in Proposition 2.1 bounds the entropy (20) which is rescaled with the boundary data. As observed in the beginning of Sec. 2, the reference function need not be constant. Hence, we choose u_r such that $u_{r|\partial\Omega_g} = u_g$ where $\partial\Omega_g$ denotes the full-state part of the boundary. Similarly, on the wall-part of the boundary, $\partial\Omega_W$, we require that the reference state has *zero normal velocity*. In 1-D that implies that $v_{r|\partial\Omega_W} = 0$.

The simplest way to achieve this, for walls and reference boundaries that are separated by a finite distance, is to let the $\rho_r = \rho_g$ and $p_r = p_g$, and let the reference velocity $v_r(x,t)$ increase smoothly and monotonically from zero at a wall boundary to v_g at the full-state boundary. *With such a $u_r(x,t)$, the entropy (3) will lead to a bound with both wall and far-field boundaries present.*

In fact, the reference function shows that both wall and full-state boundaries can be viewed as *reference boundaries* drawing boundary data from an admissible reference function.

Definition 2.2. *An admissible reference function $u_r(x,t)$ is a piecewise smooth function that satisfies the boundary conditions.*

This definition implies that $v_r = 0$ at walls and the thermodynamic variables of the reference function are arbitrary as long as they are bounded. In view of the discussion ending Section 2.2, full-state boundaries require $u_r = u_g$ since that is necessary to satisfy (16).

3. Entropy stability

Next, we turn to the implementation of the wall and full-state boundary conditions. To this end, we use a standard finite volume scheme. (Any entropy stable scheme with the summation-by-parts (SBP) property at the boundaries would do. See [19] for definitions of the SBP property.) The variables are located at the primary grid, x_i, $i = 0...N$ and the flux points are $x_{i+1/2} = (x_{i+1} + x_i)/2$. Furthermore, we take $(x_{i+1} - x_{i-1})/2 = h_i$, $i = 1...N-1$, $h_0 = (x_1 - x_0)/2$ and $h_N = (x_N - x_{N-1})/2$. For an interior point the scheme is given by,

$$(u_i)_t + \frac{f_{i+1/2} - f_{i-1/2}}{h_i} = 0 \tag{25}$$

At $x_0 = 0$, the scheme is,

$$(u_0)_t + \frac{f_{1/2} - f_0}{h_0} = \frac{1}{h_0} SAT_0, \tag{26}$$

and at $x_N = 1$,

$$(u_N)_t + \frac{f_N - f_{N-1/2}}{h_N} = \frac{1}{h_N} SAT_N. \tag{27}$$

The $SAT_{0,N}$ are simultaneous-approximation terms (see [3] and also [19]) that will be defined later. Their purpose is to enforce the boundary conditions.

We choose fluxes of the form,

$$f_{i+1/2} = \frac{f(u_{i+1}) + f(u_i) - \lambda_{i+1/2}(u_{i+1} - u_i)}{2}, \quad i = 0, 1, 2, ... \tag{28}$$

Entropy stability is obtained by choosing the artificial viscosity coefficient $\lambda_{i+1/2}$ to be suitably large. Finally,

$$f_0 = f(u_0), \quad \text{and} \quad f_N = f(u_N). \tag{29}$$

The entropy estimate is derived by multiplying (25) by $h_i w_i$.

$$w_i^T (u_i)_t + w_i^T \frac{f_{i+1/2} - f_{i-1/2}}{h_i} = 0, \tag{30}$$

and manipulating the expression to obtain,

$$h_i (U_i)_t + \frac{w_i^T + w_{i+1}}{2} f_{i+1/2} + \frac{w_i^T - w_{i+1}}{2} f_{i+1/2} - \frac{w_i + w_{i-1}}{2} f_{i-1/2} - \frac{w_i - w_{i-1}}{2} f_{i-1/2} = 0.$$

Next, the numerical entropy flux $F_{i+1/2} = \frac{w_i + w_{i+1}}{2} f_{i+1/2} - \frac{\Psi_{i+1} + \Psi_i}{2}$ is introduced, where $\Psi_i = \Psi(u_i)$ is the entropy potential. After some further manipulations, we obtain,

$$h_i (U_i)_t + F_{i+1/2} - F_{i-1/2}$$
$$+ \frac{\Psi_{i+1} - \Psi_i}{2} + \frac{w_i^T - w_{i+1}}{2} f_{i+1/2} + \frac{\Psi_i - \Psi_{i-1}}{2} - \frac{w_i - w_{i-1}}{2} f_{i-1/2} = 0$$

The assumption of entropy stability, i.e., that the artificial dissipation is sufficiently large such that

$$(w_{i+1} - w_i)^T f_{i+1/2} \leq \Psi_{i+1} - \Psi_i \tag{31}$$

holds, leads to,

$$h_i(U_i)_t + F_{i+1/2} - F_{i-1/2} \leq 0. \tag{32}$$

(Dividing through by h_i gives the local entropy inequality.) For more details on this derivation, we refer to [21].

We briefly summarise the same procedure for the left boundary scheme. That is, we multiply (26) by $h_0 w_0$ and obtain

$$h_0(U_0)_t + \frac{w_0^T + w_1}{2} f_{1/2} + \frac{w_0^T - w_1}{2} f_{1/2} - w_0 f_0 = w_0 SAT_0$$

leading to,

$$h_0(U_0)_t + \frac{w_0^T + w_1}{2} f_{1/2} - \frac{\Psi_0 + \Psi_1}{2} - \frac{w_1^T - w_0}{2} f_{1/2} + \frac{\Psi_1 - \Psi_0}{2} - w_0 f_0 + \Psi_0 = w_0 SAT_0$$

Using entropy stability of the flux $f_{1/2}$, the definition of $F_{1/2}$ and $F_0 = w_0 f_0 - \Psi_0$, we arrive at,

$$h_0(U_0)_t + F_{1/2} - F_0 \leq w_0 SAT_0. \tag{33}$$

At the right boundary, we obtain in the same way,

$$h_N(U_N)_t + F_N - F_{N-1/2} \leq w_N SAT_N. \tag{34}$$

The entropy estimate is obtained by summing (32) for $i = 1..N-1$, (33) and (34), to obtain

$$\sum_{i=1}^{N} h_i(U_i)_t \leq F_0 + w_0^T SAT_0 - F_N + w_N^T SAT_N. \tag{35}$$

3.1. Wall

We begin with the no-penetration wall boundary condition and state a stable treatment at $x = 0$.

Proposition 3.1. *If the numerical fluxes (28) are entropy stable with respect to the standard entropy $U = -\rho S$, then*

$$SAT_0 = -(f_0 - \hat{f}_0),$$
$$SAT_N = +(f_N - \hat{f}_N),$$

where $\hat{f}_{0,N} = (0, p_{0,N}, 0)^T$, leads to an entropy bound for the scheme defined in (25), (26) and (27).

Remark. $\hat{f}_{0,N}$ is obtained by inserting the boundary condition $v = 0$ into $f_{0,N}$. This flux is equal to the entropy conservative flux with respect to the states $u_{0,N} = (\rho_{0,N}, \rho_{0,N} v_{0,N}, E_{0,N})^T$ and $u_g = (\rho_{0,N}, -\rho_{0,N} v_{0,N}, E_{0,N})^T$. (That is, u_g has the same thermodynamic state as $u_{0,N}$ but the normal velocity is mirrored.) The latter view is adopted in [20,14,16].

Proof. We prove the proposition for $x = 0$. The other boundary can be handled analogously. The relevant part of the right-hand side of (35) is

$$F_0 + w_0^T SAT = F_0 - w_0^T (f_0 - \hat{f}_0) = w_0^T f_0 - \Psi_0 - w_0^T (f_0 - \hat{f}_0) = w_0^T \hat{f}_0 - \Psi_0 \tag{36}$$

Inserting expressions for w_0, $\hat{f}_0$, Ψ_0 into (36), and using the gas law $p = \rho R T$, yield,

$$F_0 + w_0^T SAT = \frac{v_0}{c_v T_0} p_0 - (\gamma - 1)\rho_0 v_0 = \frac{v_0}{c_v} \rho_0 R - (\gamma - 1)\rho_0 v_0 = 0.$$

The last equality is obtained by $\frac{R}{c_v} = \frac{c_p - c_v}{c_v} = \gamma - 1$. □

3.2. Full-state SATs

Before addressing the numerical imposition of the boundary condition given in Proposition 2.1, we make a few observations.

The R_{0g} matrix defined in (15), is identical to the one appearing in the entropy conservative diffusion coefficient for the straight line in phase space. See [21], eqn. (5.5) and the subsequent analysis where it is shown that $R_{0g} \sim |\Delta w|$.

As discussed above, the Roe-part of the boundary condition (16), i.e., $A^+_{0g}(u_0 - g) = 0$, is a non-linear version of the linear characteristic boundary conditions (10). Indeed, the linear analysis establishes the stability of small perturbations of the exact smooth solution. For small perturbation, $\Delta w << 1$ which explains why the $R_{0g}\,(\sim |\Delta w| \approx 0)$ part of (16) does not appear in the linear analysis.

However, in the non-linear case R_{0g} can not be assumed to be zero. Furthermore, there is no analytical expression, or even some sharp estimate, for R_{0g}. There are ad hoc "entropy fixes" whereby ϵI for some $\epsilon > 0$, is assumed to dominate R. This turns (16) into

$$(A^+_{0g} + \epsilon I)(u_0 - u_g) = 0. \tag{37}$$

However, such an entropy fix does not constitute a proof of entropy boundedness. To the best of our knowledge, the only rigorous way to bound R^+ is to take $\epsilon = \lambda^{LLF}$, where λ^{LLF} is the local Lax-Friedrichs diffusion coefficient obtained by taking the maximum magnitude of the eigenvalues of f_u at w_0 and w_g. Furthermore, we note that λ^{LLF} does not only dominate R, it also dominates $A^+_{0g} + R^+_{0g}H^{-1}_{0g}$ (see [21]), such that (37) can be simplified further to $\lambda^{LLF}(u_0 - u_g) = 0$.

To shed some further light on the non-linear theory of boundary conditions, we note that entropy stable schemes are really approximations of the homogenised conservation law ([2])

$$u_t + f(u)_x = (\epsilon u_x)_x, \quad \epsilon \to 0^+. \tag{38}$$

Linearly well-posed boundary conditions for (38) include Dirichlet and Robin-type conditions. Since the viscous problem requires a full set of boundary conditions, we can equally well use the simpler condition,

$$u(0,t) - \epsilon u_x(0,t) = u_g, \tag{39}$$

in place of (16). (For smooth solutions, $\epsilon \to 0$ as $h \to 0$, making (39) a Dirichlet boundary condition in the limit.) Recall the discussion ending Section 2.2 that linear theory is not equipped to provide entropy stable boundary conditions and what may seem like an overspecification in (39) is no different from (16) which is also an enforcement of weighted Dirichlet conditions.

In view of the above discussion, we consider two sets of full-state boundary conditions. One formally enforcing (16) for which we do not have closed form expressions and one enforcing (39).

Proposition 3.2. *If the numerical fluxes (28) are entropy stable with respect to the reference-function entropy, $\tilde{U}$, given by (20), then*

$$SAT = -\frac{1}{2}(A^+_{0g} + R^+_{0g}H^{-1}_{0g})(u_0 - u_g) \tag{40}$$

leads to entropy stability of (25)-(27) (w.r.t. $\tilde{U}$). Furthermore, the analytically closed condition (39) is entropy stable when enforced by,

$$SAT = -\lambda^{LLF}_{0g}(u_0 - u_g) \tag{41}$$

where λ^{LLF}_{0g} is the local Lax-Friedrichs diffusion coefficient with respect to the two states u_0 and u_g.

Remark. The viscous part of (39) does not explicitly enter (41) since it is implicitly built into the finite volume scheme. To approximate ϵu_{xx} in the boundary cell, we would need to modify (29) to become $f(u_0) - \lambda^{LLF}_{0g}(Du)_0$ where $(Du)_0$ is an approximation of $u_x(0,t)$. In doing so, we must modify the SAT to, $SAT_{mod} = -\lambda^{LLF}_{0g}(u_0 - (Du)_0 - u_g)$ in order not to change the proposed scheme. SAT_{mod} represents a weak enforcement of (39).

Proof. As in the continuous case, we add and subtract $\tilde{F}_g$ in (35) (ignoring the right boundary)

$$\frac{h}{2}(\tilde{U}_0)_t + \sum_{i>1} h(\tilde{U}_i)_t \leq \tilde{F}_0 - \tilde{F}_g + \tilde{w}_0 SAT + \tilde{F}_g \tag{42}$$

$\tilde{F}_0 - \tilde{F}_g$ can be recast in the same way as above to arrive at (18). Seeing that $\tilde{w}_g = 0$ and $\tilde{w}_0 = \Delta w_{0g}$, we have,

$$\tilde{F}_0 - \tilde{F}_g = \Delta w(A_{0g}H_{0g} + R_{0g})\Delta w \tag{43}$$

Similarly,

$$\tilde{w}_0^T SAT = -\tilde{w}_0^T \frac{1}{2}(A_{0g}^+ + R_{0g}^+ H_{0g}^{-1})(u_0 - u_g) = -\frac{1}{2}\Delta w^T (A_{0g}^+ H_{0g} + R_{0g}^+)\Delta w \tag{44}$$

The R_{0g} part is clearly bounded by the R_{0g}^+ contribution of (40) and we focus on the A_{0g} part. To this end, we diagonalise, $A_{0g} = X\Lambda X^{-1}$, and use that H_{0g} is symmetric positive definite, to obtain

$$\Delta w^T A_{0g} H_{0g} \Delta w = \Delta w^T H_{0g}^{1/2} (H_{0g}^{-1/2} X \Lambda X^{-1} H_{0g}^{1/2}) H_{0g}^{1/2} \Delta w. \tag{45}$$

Hence, the symmetric matrix $B_{0g} = A_{0g} H_{0g}$ has the same inertia as A_{0g} and (45) can be split according the sign of the eigenvalues and the positive (growing) part is cancelled by (40).

For the boundary condition (41), we only need to show that it is more diffusive than (40) in which case it bounds (43). A proof of that is found in [21]. □

3.3. Full-state boundary and wall

In the same spirit as in Sec. 2.3, we use admissible reference states as in Definition 2.2 to unify the wall and full-state boundary treatment.

Proposition 3.3. *Consider the scheme (25) with boundary schemes of the form (26) and (27). Furthermore, assume that the wall boundary conditions are implemented as in Proposition 3.1 and the full-state boundaries as in Proposition 3.2 (either (40) or (41)). Let u_r be an admissible reference function. Assume that the interior scheme is entropy stable with respect to (3) for this reference function. Then the scheme satisfies an entropy bound.*

Proof. The proof follows immediately from Proposition 3.1, Proposition 3.2 and standard entropy stability for the interior scheme. We remark that either boundary could be either a wall or a full-state boundary. □

In the one-dimensional case, with two boundary points, it is always possible to construct a continuous reference function. However, we remark that any function that is the limit of a smooth admissible reference function should do as reference function. For instance, one could construct a step-function in the reference velocity that jumps at some interior point from zero to the freestream velocity.

Note that entropy conservative fluxes, i.e., fluxes that satisfy (30) as an equality, with respect to $U = -\rho S$ are not necessarily entropy stable with respect to $\tilde{U}$ at interior points. They would if the reference function was constant but as noted above, there has to be a region (or a point) where the reference function varies. In fact, this procedure effectively precludes the use of entropy conservative schemes since it stands to reason that a scheme should be stable with respect to any admissible reference function. Hence, it would make little sense to design entropy conservative fluxes for one particular reference function. Consequently, the extension of the current theory to high-order accurate schemes, based on entropy conservative interior fluxes, is not immediate.

4. The two-dimensional scheme

To briefly demonstrate the generalisation to more than one space dimension, we consider the two-dimensional (2-D) case. (The 3-D case is analogous.) The conservation law is, $u_t + (f_1)_x + (f_2)_y = 0$ on a closed domain with piecewise smooth boundary. The variables and fluxes are given by

$$\begin{aligned} u^T &= (\rho, \rho v_1, \rho v_2, E) \\ f_1^T &= (\rho v_1, \rho v_1^2 + p, \rho v_1 v_2, v_1(E+p)) \\ f_2^T &= (\rho v_2, \rho v_2 v_1, \rho v_2^2 + p, v_2(E+p)) \end{aligned}$$

where v_i, $i = 1, 2$, are the Cartesian velocity components. The entropy is the same, $U(u) = -\rho S$ with entropy variables

$$w^T = \frac{1}{c_v}\left(-(S-\gamma) - \frac{v_1^2 + v_2^2}{2T}, \frac{v_1}{T}, \frac{v_2}{T}, \frac{-1}{T}\right).$$

Furthermore, the entropy fluxes and potentials are $F_i = -v_i U$ and $\Psi_i = (\gamma - 1)\rho v_i$, $i = 1, 2$.

We assume a triangular grid, and the unknowns are located at the vertices that in turn are connected by edges. Surrounding each point, i, is a dual volume, V_i, whose boundary is the closed arc going between the centre-of-mass and the mid-point of the edges for triangles and edges conjoined with i. (See the schematic in Fig. 1.) The union of all dual volumes cover the domain. The fluxes, $(f_{1,2})_{ik}$ are approximated at the midpoints of the edge connecting vertices i and k.

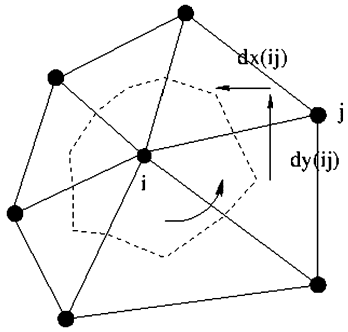

Fig. 1. The filled circles represent the variable locations. The dual volume for the point i is represented by the dashed line. dx(ij) and dy(ij) denote Δx_{ij} and Δy_{ij}.

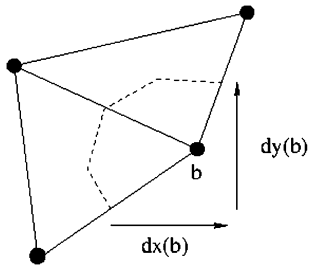

Fig. 2. The filled circles represent the variable locations. The dual volume for the boundary point b is limited by the dashed line and the outer boundary. dx(b) and dy(b) denote Δx_b and Δy_b.

The scheme is given by,

$$V_j(u_j)_t + \sum_{k\in\mathcal{N}_j} (f_1)_{jk}\Delta y_{jk} - (f_2)_{jk}\Delta x_{jk} = 0 \tag{46}$$

where j is an interior point of the mesh and $\mathcal{N}_j$ the index set of its neighbours. The Δx_{jk}, Δy_{jk} are the respective counter-clockwise coordinate distances for the (broken) facet of the dual volume that crosses the edge jk. (See Fig. 1.) An entropy stable flux at the facet is,

$$(f_1)_{jk} = \frac{f_1(u_j) + f(u_k) - A_{jk}(u_k - u_j)}{2} \tag{47}$$

where A_{jk} is a sufficiently large diffusion matrix. (The numerical flux $(f_2)_{jk}$ is defined analogously.)

Remark. On sufficiently regular grids, the finite volume scheme is second-order accurate when $A_{jk} = 0$. However, for entropy stable choices of A_{jk} (w.r.t. any entropy), the accuracy drops to first-order.

At a boundary point, b, the dual volume is defined in the same way and it is closed by the outer boundary which is also used to defined Δx_b, Δy_b. (See Fig. 2.).

The scheme for the boundary point b is,

$$V_b(u_b)_t + \sum_{k\in\mathcal{N}_b} \left((f_1)_{jk}\Delta y_{bk} - (f_2)_{jk}\Delta x_{bk}\right) + (\hat{f}_1)_b\Delta y_b - (\hat{f}_2)_b\Delta x_b = 0 \tag{48}$$

where $(\hat{f}_{1,2})_b$ are boundary flux approximations that enforce the boundary condition.

Remark. Here, we impose the boundary conditions weakly directly by choosing the flux instead of defining a SAT. The two approaches are equivalent since one can just add and subtract $(f_1)_b\Delta y_b - (f_2)_b\Delta x_b$ to obtain the associated SAT.

The entropy estimate is obtained by multiplying the scheme at all points by w_j^T, assuming that the interior scheme is entropy stable and summing. This gives in the same way as in the 1-D case,

$$\sum_{j\in\mathcal{P}} V_j(U_j)_t + \sum_{b\in\mathcal{B}} (w_b^T(\hat{f}_1)_b - (\Psi_1)_b)\Delta y_b - (w_b^T(\hat{f}_2)_b - (\Psi_2)_b)\Delta x_b = 0 \tag{49}$$

where $\mathcal{P}$ is the set of all points, and $\mathcal{B}$ is the set of boundary points. Next, we choose the boundary fluxes, $(\hat{f}_{1,2})_b$ for the two types of boundaries.

Remark. Tadmor's shuffle condition for two neighbouring points i, k, required for internal entropy stability, is,

$$\frac{w_i^T + w_k^T}{2}(f_1 \Delta y_{ik} - f_2 \Delta x_{ik}) - \left((\bar{\Psi}_1)_{ik} \Delta y_{ik} - (\bar{\Psi}_2)_{ik} \Delta x_{ik})\right) \leq 0$$

where $(\bar{\Psi}_{1,2})_{ik} = \frac{(\Psi_{1,2})_i + (\Psi_{1,2})_k}{2}$.

4.1. Wall

The boundary condition at b is $v_n = (v_1, v_2) \cdot (n_1, n_2)_b = 0$, where $(n_1, n_2)_b$ is the outward pointing boundary normal. In the scheme, we use the (scaled) approximation $(n_1, n_2)_b = (\Delta y_b, -\Delta x_b)$.

The boundary flux without the boundary condition imposed, is (dropping the subscript b)

$$n_1 f_1 + n_2 f_2 = n_1 \begin{pmatrix} \rho v_1 \\ \rho v_1^2 + p \\ \rho v_1 v_2 \\ v_1(E+p) \end{pmatrix} + n_2 \begin{pmatrix} \rho v_2 \\ \rho v_1 v_2 \\ \rho v_2^2 + p \\ v_2(E+p) \end{pmatrix} = \begin{pmatrix} \rho v_n \\ \rho v_1 v_n + n_1 p \\ \rho v_2 v_n + n_2 p \\ v_n(E+p) \end{pmatrix} \tag{50}$$

Using $v_n = 0$ results in the numerical boundary flux,

$$n_1(\hat{f}_1)_b + n_2(\hat{f}_2)_b = \begin{pmatrix} 0 \\ n_1 p \\ n_2 p \\ 0 \end{pmatrix}. \tag{51}$$

With this boundary flux, it is straightforward to verify that

$$(w_b^T(\hat{f}_1)_b - (\Psi_1)_b)\Delta y_b - (w_b^T(\hat{f}_2)_b - (\Psi_2)_b)\Delta x_b = 0$$

at all boundary points in (49). We summarise the results in a proposition.

Proposition 4.1. *Assume that the scheme (46)-(48) is equipped with entropy stable interior fluxes. Then the numerical flux (51) leads to an entropy bound w.r.t. (3) with $v_r = 0$. Furthermore, (51) enforces an approximation of the no-penetration wall boundary condition.*

4.2. Full-state boundary

We only consider the generalisation of the Dirichlet (Lax-Friedrichs) option for far-field boundary condition since that is the only practically viable choice.

Proposition 4.2. *Assume that the interior fluxes of the scheme (46)-(48) are entropy stable. Furthermore, let $\lambda_b^{LLF} = \max(\{|v_n| + c\}_{0,b})$, where v_n is the velocity projected on the (approximate) normal direction. Then the following boundary flux for full-state boundary points, b,*

$$n_1(\hat{f}_1)_b + n_2(\hat{f}_2)_b = n_1 f_1(u_b) + n_2 f_2(u_b) - \lambda_b^{LLF}(u_b - u_g) \tag{52}$$

leads to entropy stability with respect to (3) with $u_r = u_g$.

Proof. The proof is analogous to the 1-D case. □

4.3. Compatibility of walls and full-state boundaries

In more than one space dimension, there are more possibilities to combine different boundary types. The simplest case is an object in freestream surrounded by a far-field boundary. In this case, it is straightforward to construct a smoothly varying reference function with zero normal velocity at the object and freestream velocity at the boundary with the freestream thermodynamic state being constant everywhere. (This is the obvious generalisation of the 1-D case.)

However, in the case of e.g. channels flows, one might have a wall boundary adjacent to inlets and/or outlets. (Here, modelled with information about the full state vector.) To handle this, we define a compatibility relation.

Definition 4.3. *Assume that the boundary $\partial\Omega$ of the computational domain Ω is piecewise differentiable with a finite number of corners. If the admissible reference function can be extended outside the domain such that it is continuous in a neighbourhood of the corner, we say that the boundary conditions are* compatible.

At the corner between a wall and a full-state boundary, compatibility means that the reference velocity at the full-state boundary is parallel to the wall at the corner and the thermodynamic variables and remaining velocity components are continuous across the corner.

Furthermore, we note that the reference state need not be constant along a boundary piece. This allows for e.g. a varying (in time and space) velocity field at an inlet.

Since the reference function provides the boundary data, its smoothness properties affect the smoothness of the solution. Our notion of compatibility is the same as in [6] but expressed differently. With higher compatibility, i.e., higher smoothness of u_r, higher smoothness of the solution is obtained (in the absence of shocks etc.).

However, we also note that the scheme will remain entropy stable even if the reference function is discontinuous and incompatible, as long as the reference function can be constructed as the limit of smooth and compatible reference functions.

4.4. Some remarks on the affine entropy

Our boundary procedure along with internal entropy stability (with respect to *any* entropy) guarantees entropy stability of the initial-boundary value problem. However, we stress that if entropy stable fluxes (w.r.t. any entropy) are used, the reference function is not explicitly used in the scheme (apart from as boundary data) when the Dirichlet (Lax-Friedrichs) boundary condition (39) is used. Indeed, it would be odd if the scheme was depending on a largely arbitrary auxiliary function.

On the other hand, entropy stable interior schemes are very diffusive and it might be possible to be a bit more subtle. Since the reference function is essentially arbitrary in the interior, the scheme should be designed for whatever transition the velocity in the reference function takes. The worst case is if it transitions within one cell. Thus, any of the cells should be designed to handle the transition, but this might be less diffusive than being able to handle any entropy. (It amounts to bounding essentially two, rather than infinite number of, entropies.)

Finally, we have only considered wall and full-state boundaries but it should be clear that any entropy stable boundary conditions can be viewed as *reference boundary conditions* making the *reference function* central to entropy stability of initial-boundary value problems. We have introduced it as a function designed to satisfy the boundary conditions. However, one can take the opposite view that the entropy is bounded with respect to a global reference function that provides the boundary data.

5. Numerical experiments

We consider two numerical experiments. The first is the interaction between a strong vortex and a subsonic outflow boundary with constant freestream data. This is a model of a far-field boundary hit by vortices emanating from an object, or it can be seen as a model of an outlet of a channel where flow structures are significantly different from the boundary data.

The second problem is the flow around a NACA0012 aerofoil, which tests the robustness of both a wall boundary and the far-field boundaries that are deliberately close to the aerofoil such that shocks impinge on them.

5.1. Simulation of inviscid vortex

To test the far-field/outlet boundary conditions, we have initiated the flow with an isentropic vortex at the centre of the two-dimensional domain $[0,1]^2$. The domain is discretised by a randomly perturbed triangulated Cartesian grid with 100×100 points. The finite volume scheme, (46) and (48), was implemented and marched in time with a standard 3rd-order Strong-Stability Preserving Runge-Kutta scheme and a timestep $\Delta t = 2.8653295128939830E-006$ (that is a CFL≈ 1).

The freestream has a Mach-number of 0.1 and the remaining freestream data and the vortex definition are given in Appendix A. This Mach number makes the right boundary a subsonic outflow for which Dirichlet boundary conditions imply an overspecification according to linear theory (but not according to the present non-linear theory).

The vortex is strong such that the mismatch with the freestream data on the outflow is substantial causing a violent interaction. Although the scheme is linearly stable even without artificial diffusion (see [9]), the vortex is so strong that linear theory is not valid. Hence, some artificial diffusion must be added to stabilise the flow. (This has nothing to do with boundaries since the instabilities occur long before any boundary interaction.) We add 5% of the local Lax-Friedrichs diffusion which seems to be about the least possible.

In summary, the resolution in space, time and the small amount of artificial diffusion makes the numerical errors from the interior negligible compared to the interaction with the boundary. This can be seen in Fig. 3 which is a snapshot of the solution at $t = 0.005$, well before any interaction with the boundary. The figure depicts an undisturbed vortex.

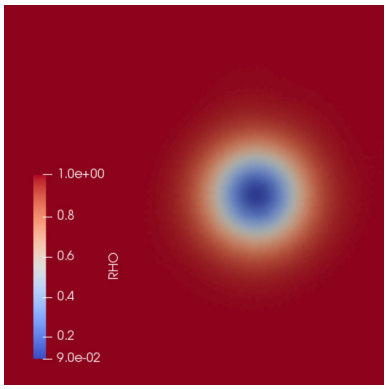

Fig. 3. rho, $t = 0.005$.

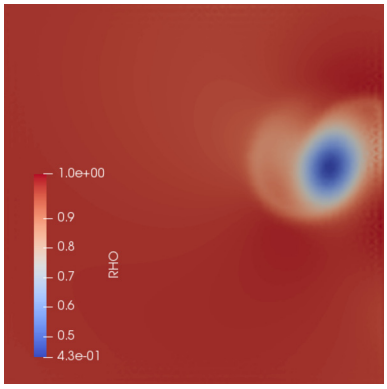

Fig. 4. rho, $t = 0.015$.

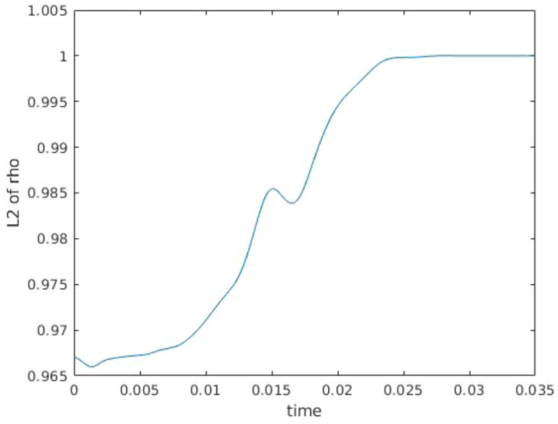

Fig. 5. L^2 norm of ρ.

In Fig. 4, the vortex has reached the boundary and it is distorted by the mismatch with the boundary data. We stress that this is expected. Only if the analytical vortex solution is used as boundary data will the vortex pass through the boundary undisturbed. For all other boundary data and boundary conditions, there will be reflections. (See e.g. [15] that shows a similar behaviour for a scheme with characteristic boundary conditions and freestream data.)

Finally, we show the time evolution of the L^2-norm of the density (see Fig. 5). At $t = 0.015$ the interaction between the vortex and the boundary, which is causing reflections, is clearly seen. However, at $t = 0.025$ the reflected disturbances have been swept out of the domain and the density has settled on the freestream value.

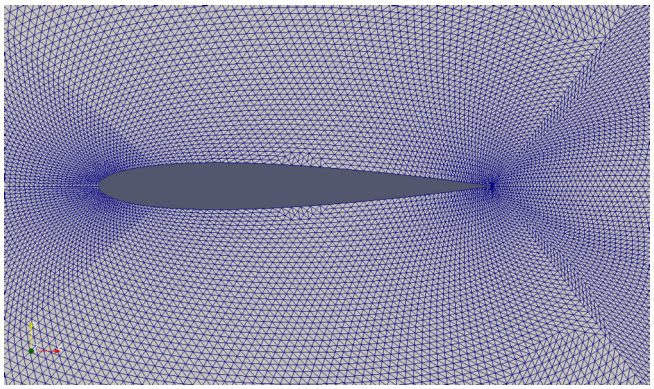

Fig. 6. Close up of the grid near the aerofoil.

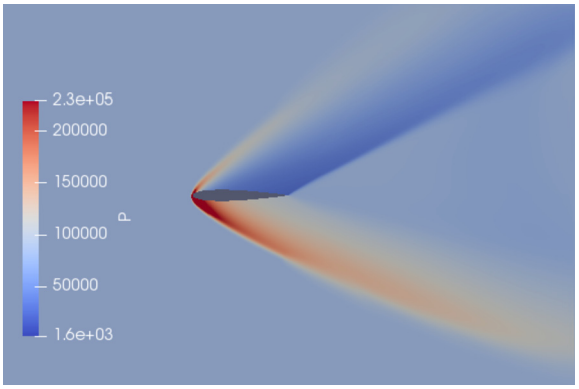

Fig. 7. Pressure distribution. $Ma_\infty = 2.5$ at 10 degrees angle of attack.

5.2. NACA0012

In this test, we consider a NACA0012 aerofoil with a triangular grid consisting of 39600 nodes. Part of the grid is depicted in Fig. 6. It was generated from a (not very smooth) structured multi-block grid. In order to test the far-field boundary conditions, we have chosen the computational domain to be small, $[-2, 4] \times [-2, 2]$. (We acknowledge that this is not a physically accurate model of an aerofoil in a freestream.) We ran the finite volume code with a CFL of 1 and the 3rd-order SSP-RK time marching in time. We use scalar artificial diffusion, namely 0.3 times the Lax-Friedrichs diffusion, which is less diffusion than the Roe scheme. It is too little to be guaranteed to be entropy stable and thus it will put more strain on the boundary conditions than an entropy stable choice would. The flow is initiated with a constant freestream with Mach-number 2.5 and 10 degrees angle of attack in the entire domain, i.e., a severe mismatch between boundary data and initial conditions at the wall.

Despite the rather small diffusion and the violent startup, the code ran stably and produced the solution depicted in Fig. 7.

Furthermore, we draw the attention to the far-field boundaries and in particular the supersonic outflow behind the aerofoil. Since the domain is small (in Fig. 7 the entire domain is shown) and the grid is relatively fine near the outflow, the flow is still fairly resolved and not overly diffused. Hence, the non-linear waves extend all the way to the far-field boundaries and there is a substantial mismatch between the solution and the freestream data which is enforced through the boundary condition.

Recall that linear theory suggests that no boundary conditions are specified near the outflow. Here, we specify all 4 variables weakly using (39) and yet there are no visible artificial boundary layers caused by our procedure. (However, we do not claim that the solution close to the aerofoil is unaffected by the close proximity of the outer boundaries.)

6. Conclusions

We have analysed entropy stability for the Euler equations with wall and full-state boundary conditions (far-field, inlet, outlet) with respect to the Navier-Stokes entropy. In particular, we have proposed a stable weak enforcement of the no-penetration condition and proposed novel closed-form Robin-type boundary conditions (39) (and the formally stable but

not on closed form (16)) along with stable numerical approximations. This was accomplished by constructing an affine transformation of the Navier-Stokes entropy with respect to a *reference function* that satisfies the boundary conditions.

We have also discussed the linear theory for the number of necessary boundary conditions, that "paradoxically" implies entropy stability for a wall but not at the far-field. However, the linear theory provides boundary conditions for perturbations of a supposedly known and smooth background field. Our non-linear analysis confirms this behaviour: In (16) the R_{0g}^{+} is negligibly small for a very smooth solution and the remaining Roe part (A_{0g}^{+}) enforces characteristic boundary conditions in accordance with linear theory. On the other hand, at a wall the no-penetration boundary condition is the proper condition for *both* perturbations and the background field making it valid for both the linear and non-linear analysis.

However, we also claim that *non-linearly averaged characteristic boundary conditions (including (16) and other Roe-type averages) always enforce as many boundary conditions as variables.* This is realised by noting that only when *all components of the solution vector equal their counterpart of the boundary data is the boundary condition satisfied.*

Since the full data vector is anyway enforced, and since analytical expressions for R_{0g} in (16) are unavailable making the boundary condition difficult to use in practice, we advocate to use the simpler (39) at full-state boundaries. To further motivate this suggestion, we pointed out that the boundary condition (39) is consistent with viscous limits. Finally, we demonstrated numerically that the proposed wall and full-state boundary treatment (39) are exceptionally robust.

Although, we have derived a finite volume scheme as an example of how to use these boundary conditions, they are not limited to such schemes. The key features of the scheme are local entropy stability and the summation-by-parts (SBP) property. The boundary conditions are applicable to any such scheme, be it a SBP finite difference, discontinuous Galerkin or a spectral collocation element scheme.

The generalisation of the far-field boundary conditions to Robin-type for the Navier-Stokes equations (similar to [15]) should be straightforward provided that the internal discretisation of the viscous terms is entropy stable.

CRediT authorship contribution statement

I am the sole author.

Declaration of competing interest

The authors declare that they have no known competing financial interests or personal relationships that could have appeared to influence the work reported in this paper.

Appendix A. Euler vortex

The centre of the vortex is located at $(x_c, y_c) = (0.5, 0.5)$. The freestream conditions are given by

$$Ma = 0.1 \text{ (in the x-direction)}, \quad \rho_\infty = 1, \quad T_\infty = 273.15,$$

with the physical constants

$$R_g = 287.15 \text{ (ideal gas constant)}, \quad \text{and } \gamma = 1.4 \quad \text{adiabatic exponent.}$$

The radius of the vortex is $R_v = 0.1$ and $\beta = 20$ (strength). The functions defining the vortex are,

$$\begin{aligned} f(x,y) &= (x-x_c)^2 + (y-y_c)^2)/R_v^2 \\ dv_1(x,y) &= -(v_\infty \beta) \cdot ((y-y_c)/R_v) \cdot exp(-f/2) \\ dv_2(x,y) &= (v_\infty \beta) \cdot ((x-x_c)/R_v) \cdot exp(-f/2) \\ dT(x,y) &= 0.5 \cdot (v_\infty \beta)^2 \cdot exp(-f)/c_p \end{aligned}$$

and the field variables are,

$$\begin{aligned} \rho &= \rho_\infty ((T_\infty - dT)/T_\infty)^{1/(\gamma-1)}, \\ \rho u &= \rho \cdot (u_\infty + dv_1), \\ \rho v &= \rho \cdot dv_2, \\ \frac{p}{\gamma - 1} &= \rho R_g (T_\infty - dT). \end{aligned}$$

References

[1] S. Abarbanel, D. Gottlieb, Optimal time splitting for two- and three-dimensional Navier-Stokes equations with mixed derivatives, J. Comput. Phys. (1981).
[2] F. Du Bois, P. Le Floch, Boundary conditions for nonlinear hyperbolic systems of conservation laws, J. Differ. Equ. 71 (1) (1988) 93–122.
[3] M.H. Carpenter, D. Gottlieb, S. Abarbanel, Time-stable boundary conditions for finite-difference schemes solving hyperbolic systems: methodology and application to high-order compact schemes, J. Comput. Phys. 111 (2) (1994).
[4] P. Dutt, Stable boundary conditions and difference schemes for Navier-Stokes equations, SIAM J. Numer. Anal. 25 (2) (1988) 245–267.
[5] E. Feireisl, A. Novotný, Singular Limits in Thermodynamics of Viscous Fluids, 2nd ed., Birkhäuser, 2017.
[6] B. Gustafsson, H.-O. Kreiss, J. Oliger, Time Dependent Problems and Difference Methods, John Wiley & Sons, Inc., 1995.
[7] B. Gustafsson, A. Sundström, Incompletely parabolic systems in fluid dynamics, SIAM J. Appl. Math. (1978).
[8] J.S. Hesthaven, D. Gottlieb, A stable penalty method for the compressible Navier-Stokes equations: I. Open boundary conditions, SIAM J. Sci. Comput. (1996).
[9] J. Nordström, K. Forsberg, C. Adamsson, P. Eliasson, Finite volume methods, unstructured meshes and strict stability for hyperbolic problems, Appl. Numer. Math. 45 (4) (June 2003) 453–473.
[10] J. Nordström, The influence of open boundary conditions on the convergence to steady state for the Navier–Stokes equations, J. Comput. Phys. 85 (1989).
[11] J. Nordström, Accurate solution of the Navier–Stokes equations despite unknown outflow boundary data, J. Comput. Phys. 120 (1995).
[12] J. Nordström, The use of characteristic boundary conditions for the Navier-Stokes equations, Comput. Fluids 24 (5) (1995) 609–623.
[13] J. Nordström, M. Svärd, Well posed boundary conditions for the Navier-Stokes equations, SIAM J. Numer. Anal. 43 (3) (September 2005) 1231–1255.
[14] M. Parsani, M.H. Carpenter, E.J. Nielsen, Entropy stable wall boundary conditions for the three-dimensional compressible Navier-Stokes equations, J. Comput. Phys. 292 (2015) 88–113.
[15] M. Svärd, M.H. Carpenter, J. Nordström, A stable high-order finite difference scheme for the compressible Navier-Stokes equations, far-field boundary conditions, J. Comput. Phys. 225 (2007) 1020–1038.
[16] M. Svärd, M.H. Carpenter, M. Parsani, Entropy stability and the no-slip wall boundary condition, SIAM J. Numer. Anal. 56 (1) (2016) 256–273.
[17] M. Svärd, S. Mishra, Entropy stable schemes for initial-boundary-value conservation laws, Z. Angew. Math. Phys. 63 (2012) 985–1003.
[18] M. Svärd, J. Nordström, A stable high-order finite difference scheme for the compressible Navier-Stokes equations, no-slip wall boundary conditions, J. Comput. Phys. 227 (2008) 4805–4824.
[19] M. Svärd, J. Nordström, Review of summation-by-parts schemes for initial–boundary-value problems, J. Comput. Phys. 268 (2014) 17–38.
[20] M. Svärd, H. Özcan, Entropy stable schemes for the Euler equations with far-field and wall boundary conditions, J. Sci. Comput. 58 (1) (2014) 61–89.
[21] E. Tadmor, Entropy stability theory for difference approximations of nonlinear conservation laws and related time-dependent problems, Acta Numer. (2003) 451–512.